JOURNAL OF APPLIED ELECTROCHEMISTRY 20 (1990) 672–676

Electrochemical studies with tin electrodes in citric acid solutions

B. F. GIANNETTI, P. T. A. SUMODJO, T. RABOCKAI

Instituto de Quimica da USP, Caixa Postal 20.780, 01498-São Paulo, SP, Brazil

Received 6 April 1989; revised 15 October 1989

The electrochemical behaviour of tin in 0.5 M citric acid solution (pH = 1.8) was studied by means of the potentiodynamic method. The *E-I* profiles show an anodic current peak associated with a dissolution of the metal and the formation of a passivating film, and two cathodic current peaks which are related to the reduction of soluble Sn(II) species and reduction of the film. During the potential sweep in the cathodic direction, an anodic current peak can be observed and is interpreted in terms of a reactivation process. The data suggest that the passivation of tin in this medium occurs by a dissolution-precipitation mechanism. Depending on the potential sweep rate, the process is controlled either by mass transport or by the solution resistance in the pores of the film.

1. Introduction

Tin is a moderately corrosion resistant metal, widely employed in the production of tin can, soft solders, bronze and other alloys. The knowledge of its electrochemical behaviour is, therefore, of considerable interest. While numerous investigations of the behaviour of tin in alkaline solutions have been reported [1–17], relatively few papers deal with the anodic dissolution of tin in acid solutions [18–27]. Corrosion under simulated food storage conditions in tinned containers [28–32] has been investigated, as has the effect of antimony on the corrosion of tin in deaerated citric acid [32] and the behaviour of the tin-steel couple in air-free citric acid solutions [31].

The present paper examines the potentiodynamic behaviour of tin in deaerated citric acid solutions.

2. Experimental details

The working electrode, a disc with an apparent area of 0.8 mm^2, was constructed following the procedure described by Sharpe and Meibhur [33]. A platinized platinum electrode was used as the counter electrode, and a reversible hydrogen electrode (RHE), placed in the same solution, was used for reference. All potentials are quoted with respect to this electrode.

The electrolyte was a 0.5 M citric acid solution, which corresponds to a pH = 1.8. It was prepared with analytical grade reagent and triple distilled water and stored at low temperature to avoid decomposition.

Preceeding each experiment the working electrode was polished with 600 emery-paper and suspensions of alumina powder (0.3 μm and 0.02 μm, respectively), following the usual metallographic procedure [34]. The electrode was then rinsed with distilled water, dipped in the solution which had previously been deaerated with purified nitrogen, and then cathodized at −0.9 V for 5 minutes to reduce any surface oxide. Hydrogen bubbles formed during the cathodic polarization were removed by purging with nitrogen for 30 s. After a 30 s rest an anodic potential sweep was applied to the electrode. Each experiment was repeated at least twice, and the potentiodynamic curves showed good reproducibility.

The temperature was maintained at (25 ± 1)° C.

3. Results and discussion

Fig. 1 shows a typical potentiodynamic *E-I* curve for tin in 0.5 M citric acid solution. Hydrogen evolution occurs for potentials more negative than −0.5 V, and oxygen evolution begins at 3.0 V. An anodic current peak, a_I, characteristic of passivation processes, appears around 0.0 V. At more positive potentials a low intensity stationary current, which corresponds to the passive state, is observed. Since oxygen evolution occurs, it may be assumed that a conducting film is formed. During the reverse scan a small cathodic current peak, c_I, appears near the potential where hydrogen evolution initiates.

Figs 2, 3 and 4 show the potentiodynamic profiles recorded at 0.1 $V s^{-1}$, for different anodic end point potentials ($E_{\lambda,a}$). When $0.2\,V < E_{\lambda,a} < 0.7\,V$ the anodic current peak a_{II} is observed during the reverse potential scan (Figs 2b and 3b). This peak suggests the occurrence of a reactivation process which will be discussed later. A cathodic current peak, c_{II}, is observed for $E_{\lambda,a}$ values between −0.1 V and 0.7 V. Fig. 2 shows an increase of that current peak when $E_{\lambda,a}$ is increased. In the range $0.3\,V < E_{\lambda,a} < 0.7\,V$, current peak c_{II} diminishes with increasing $E_{\lambda,a}$; and for $E_{\lambda,a} \simeq 0.7\,V$ the appearance of cathodic current peak c_I is apparent (Fig. 3b). As $E_{\lambda,a}$ varies from 0.7 V to 1.1 V, peak c_{II} gradually disappears and peak c_I prevails (Fig. 3b). The nature of these peaks will be discussed later.

With increasing sweep rate the peak current at a_I

0021-891X/90 $03.00 + .12

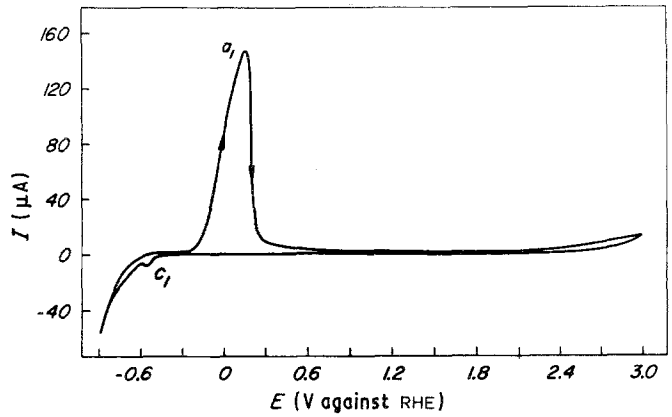

Fig. 1. Potentiodynamic *E-I* profile of tin in 0.5 M citric acid; $v = 0.1\,V\,s^{-1}$, $A = 0.8\,mm^2$.

(I_{p,a_I}) increases, and the corresponding potential (E_{p,a_I}) shifts to more positive values; the peak current at a_{II} ($I_{p,a_{II}}$) diminishes and disappears for potential sweep rates, v, higher than $0.5\,V\,s^{-1}$, the corresponding peak potentials ($E_{p,a_{II}}$) shift to more negative values.

Fig. 5 shows that the anodic to cathodic charge ratio (Q_a/Q_c) is greater than unity at low potential sweep rates. This fact, and the shape of the cyclic voltammogram, (Fig. 1), suggest an active dissolution-passivation process [35]. Therefore, the anodic current peak is indicative of two processes: the dissolution of the metal and the formation of a film.

The cyclic voltammograms recorded with stirred and unstirred solution, at $v = 0.1\,V\,s^{-1}$ and $12\,V\,s^{-1}$ are compared in Figs 6 and 7, respectively. At low values of v, current peak a_I increases when the solution is stirred indicating a dissolution process. At high sweep rates the hydrodynamic perturbation does not change the profile of peak a_I, presumably the sweep rate is so fast as to negate the effects of the enhanced hydrodynamics.

The potentiodynamic oxidation of tin in alkaline solutions results in an *E-I* profile with two anodic current peaks. According to several authors [5, 11], SnO or $Sn(OH)_2$ is formed in the first step, and passivation with the formation of SnO_2 or $Sn(OH)_4$ occurs successively. The formation of SnO_2 by direct oxidation of the metal is not thermodynamically and kinetically favourable [16]. Since peak a_I is also increased when Sn^{2+} ions are added to the solution (Fig. 8), one may assume that dissolution of tin in citric acid occurs in two steps and involves a Sn(II) species.

It is well known that tin undergoes hydrolysis at pH = 1.5 [36, 37]; thus, it can be assumed that the main steps of the anodic process are:

$$Sn \longrightarrow Sn(II) + 2e$$

$$Sn(II) \rightleftharpoons Sn(IV) + 2e$$

$$Sn(IV) + 4H_2O \rightleftharpoons Sn(OH)_4 + 4H^+$$

$$Sn(OH)_4 \longrightarrow SnO_2 \cdot xH_2O$$

The Sn(II) and Sn(IV) ions can form still unkown species, which would yield $Sn(OH)_4$. Since this hydroxide is highly insoluble (solubility product, $K_{ps} = 1 \times 10^{-59}$) [36], it precipitates giving rise to a passivating film. The last step is that of $Sn(OH)_4$ dehydration yielding SnO_2. For this reaction $\Delta G = -42\,kJ\,mol^{-1}$ [38], therefore the formation of the $SnO_2 \cdot xH_2O$ species is thermodynamically favoured.

Figs 2b and 3a show that peak a_{II} appears during the negative scan, for $0.2\,V < E_{\lambda,a} < 0.7\,V$, and $v = 0.1\,V\,s^{-1}$. Experiments at different potential sweep rates, reversing the potential scan after peak a_I is formed, show that current peak a_{II} diminishes as v increases (Fig. 9). Fig. 10 shows that for successive potential scans in a potential range which allows the formation of current peak a_{II} and does not allow the reduction to occur, peak a_I always appears. However, if $E_{\lambda,a}$ is such that current peaks a_{II} and c_I are not formed, the electrode remains passivated during the successive scans (Fig. 11a). These facts suggest that peak c_I is related to the reduction of the film, and the reactivation process can be attributed to the

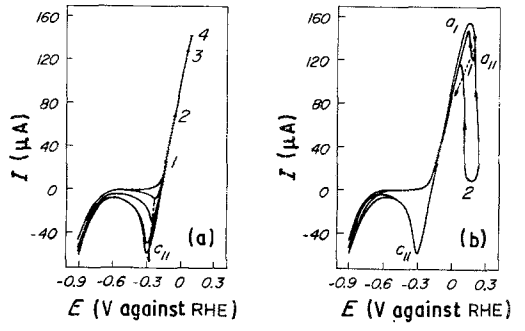

Fig. 2. The influence of the anodic switching potential, $E_{\lambda,a}$, on the potentiodynamic profile; $v = 0.1\,V\,s^{-1}$; $A = 0.8\,mm^2$. (a): (1) −0.14; (2) −0.06; (3) 0.06; (4) 0.09. (b): (1) 0.21; (2) 0.26.

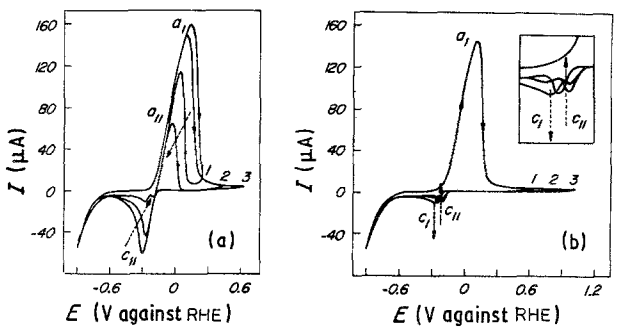

Fig. 3. The influence of $E_{\lambda,a}$ on the potentiodynamic *E-I* profile; $v = 0.1\,V\,s^{-1}$; $A = 0.8\,mm^2$. (a): (1) 0.26; (2) 0.42; (3) 0.63. (b): (1) 0.63; (2) 0.84; (3) 1.05; peaks c_I and c_{II} region is detailed in the insert.

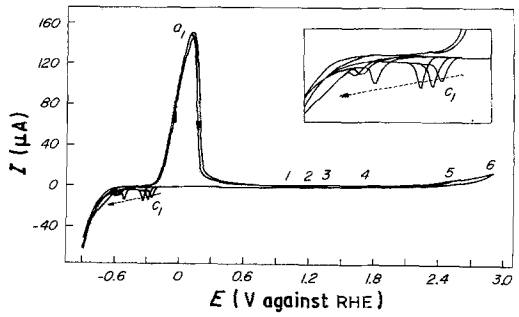

Fig. 4. The influence of $E_{\lambda,a}$ on the potentiodynamic *E-I* profile; $v = 0.1\,V\,s^{-1}$; $A = 0.8\,mm^2$; (1) 1.05; (2) 1.18; (3) 1.38; (4) 1.77; (5) 2.52; (6) 2.91. Peak c_I region is detailed in the insert.

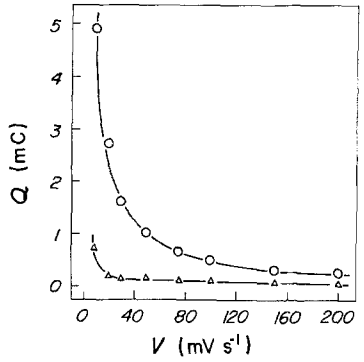

Fig. 5. The variation of the total charge with potential scan rate; (○) anodic; (△) cathodic.

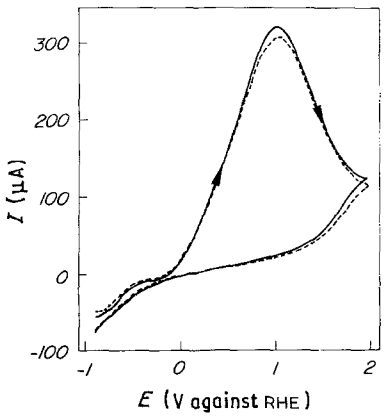

Fig. 7. The influence of stirring on the potentiodynamic *E-I* profile; $v = 12\,V\,s^{-1}$; $A = 0.8\,mm^2$; (– –) without stirring, (——) with stirring.

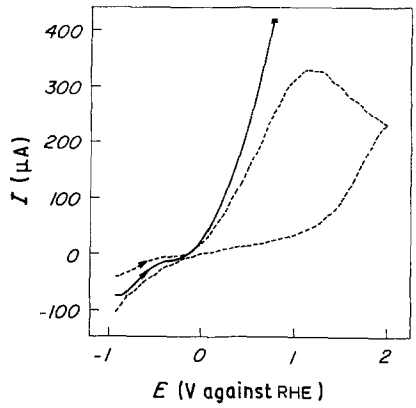

Fig. 8. Potentiodynamic profile: $v = 16\,V\,s^{-1}$; $A = 0.8\,mm^2$; (——) Sn^{2+} present in the solution, (– –) Sn^{2+} absent.

rupture of the film [39] and/or the active dissolution of the metal in the presence of that film [9].

In Fig. 6 the potentiodynamic *E-I* profiles for stirred and unstirred solutions are compared. It is seen that hydrodynamic perturbation does not change current peak, c_I. This behaviour may be explained assuming that current peak c_I is related to the reduction reaction of the interfacial species. Since peak c_I shifts to more negative potentials as $E_{\lambda,a}$ is increased (Fig. 4), the reduction of the passive film takes place after the occurrence of some ageing of that film.

The cyclic voltammograms obtained when the electrode is subject to a repetitive triangular potential sweep between $E_{\lambda,a} = 1.5\,V$, which corresponds to a passive state, and $E_{\lambda,c} = -0.22\,V$, just before the appearing of peak c_I (Fig. 11a), show that peak c_I is related to the reduction of a passive film. Fig. 11b shows the voltammogram corresponding to the last potential scan with $E'_{\lambda,c} = -0.9\,V$. The presence of current peaks c and a, indicate that the film is reduced.

Current peak c_{II} changes with stirring (Fig. 6a), showing that it corresponds to the reduction of tin species present in the solution.

Current peak a_I varies linearly with $v^{1/2}$ for sweep rates in the range $0.01\,V\,s^{-1} < v < 0.2\,V\,s^{-1}$ (Fig. 12). From the observations related to peak a_I, this linear

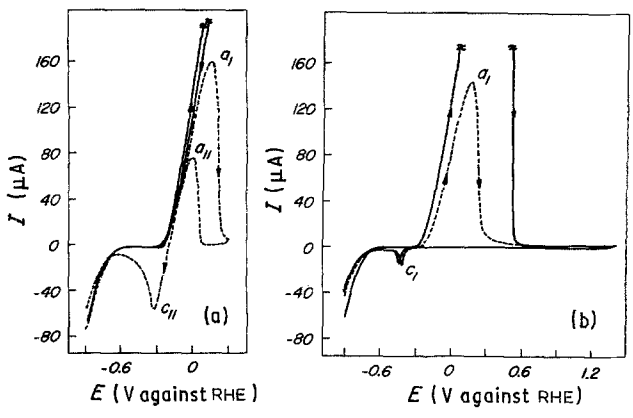

Fig. 6. The influence of stirring on the potentiodynamic *E-I* profile; $v = 0.1\,V\,s^{-1}$; $A = 0.8\,mm^2$; (– –) without stirring, (——) with stirring; (a) $E_{\lambda,a} = 0.34\,V$, (b) $E_{\lambda,a} = 1.5\,V$.

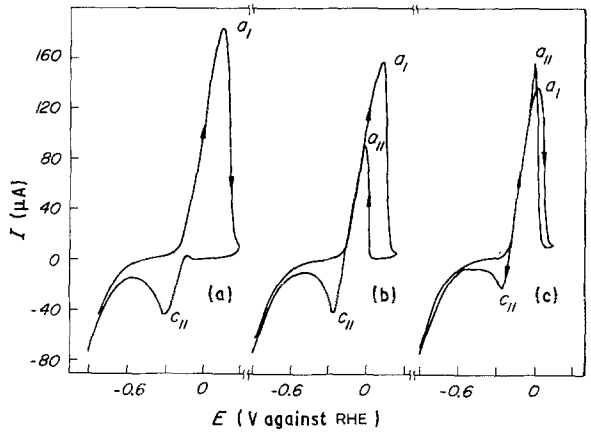

Fig. 9. Cyclic voltammograms with different potential sweep rates at the a_{II} current peak region; $A = 0.8\,mm^2$; (a) $v = 0.2\,V\,s^{-1}$; (b) $v = 0.075\,V\,s^{-1}$; (c) $v = 0.03\,V\,s^{-1}$.

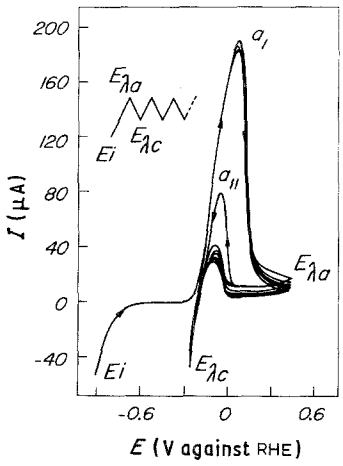

Fig. 10. Cyclic voltammograms obtained with the schematized perturbation program; $v = 0.1\,V\,s^{-1}$; $A = 0.8\,mm^2$; $E_i = -0.9\,V$; $E_{\lambda,a} = 0.52\,V$; $E_{\lambda,c} = E_f = -0.22\,V$.

relation suggest that at low potential sweep rates this peak is essentially originated by a dissolution process controlled by diffusion. A non-protective film is possibly formed [18].

It is observed in Fig. 13 that both, I_{p,a_I} and E_{p,a_I} vary linearly with the square root of the potential sweep rate for $v > 8\,V\,s^{-1}$. Therefore, for high sweep rates, the formation of the insoluble film can be described by the dissolution-precipitation mechanism, controlled by the solution resistance in the pores of the film, as was proposed by Müller and Calandra [35, 40]. According to this model, the resistance is relatively small until 99% of the electrode surface is covered by the film. Therefore, it seems reasonable to assume that, at the current peak potential, the surface is practically covered by the film. Since the recorded anodic current is a result of two distinct contributions, the degree of coverage cannot be evaluated from the voltammograms. This evaluation is done by means of the following equation [41]:

$$I_p = \left(\frac{nF\rho\kappa}{M}\right)^{\frac{1}{2}} A(1 - \theta_p)v^{\frac{1}{2}} \qquad (1)$$

where M is the mass of the film formed by the flow of nF Coulombs of charge, ρ is the film density, κ the specific conductivity of the solution, A the electrode area and the surface coverage. Assuming that the film

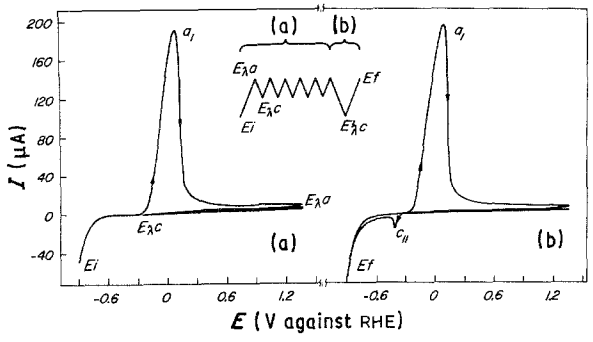

Fig. 11. Cyclic voltammograms obtained with the schematized perturbation program; $v = 0.1\,V\,s^{-1}$; $A = 0.8\,mm^2$; $E_i = -0.9\,V$; $E_{\lambda,a} = E_f = 1.5\,V$, $E_{\lambda,c} = -0.22\,V$; $E'_{\lambda,c} = -0.9\,V$.

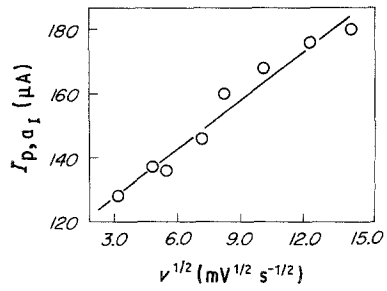

Fig. 12. Plots of I_p against $v^{\frac{1}{2}}$ for peak a_I; $v < 0.2\,V\,s^{-1}$; $A = 0.8\,mm^2$.

formed initially consists basically of SnO_2 [18], the following numerical values are used in Equation 1: $\rho = 6\,g\,cm^{-3}$, $\kappa = 6 \times 10^{-3}\,S\,cm^{-1}$ and $A = 8 \times 10^{-3}\,cm^2$.

From the slope of the straight line in Fig. 13 $I_{p,a_I}/v^{\frac{1}{2}} = 84.6 \times 10^{-6}(CS)^{\frac{1}{2}}$ is obtained. Introducing these values in Equation 1 results in $\theta_p = 0.9989$. Therefore, the Müller model is suitable for describing the passivation of tin in citric acid media, in potentiodynamic conditions at high sweep rates.

In Fig. 14 the linear variation of the half peak width potential ($\Delta E_{a_I,\frac{1}{2}}$) with v is shown. The linear relationships illustrated in Figs 13 and 14 are predicted by the nucleation-growth model for potentiodynamic conditions when a rapid and irreversible nucleation process occurs.

4. Conclusions

The potentiodynamic oxidation of tin in citric acid medium, despite the simplicity of the *E-I* profile obtained, is a complex process. The anodic current is initially related to the formation of soluble Sn(II) species, which are subsequently oxidised to Sn(IV). The sharp fall of the current at the a_I current peak is attributed to the formation of a passivating film, originated by the hydrolysis of Sn(IV). At low potential

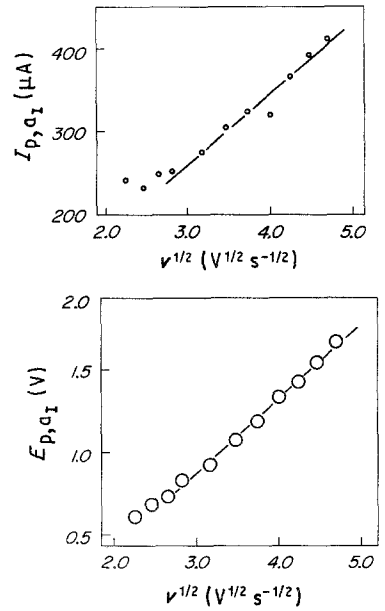

Fig. 13. Plots of I_p and E_p against $v^{\frac{1}{2}}$ for peak a_I; $v > 8\,V\,s^{-1}$; $A = 0.8\,mm^2$.

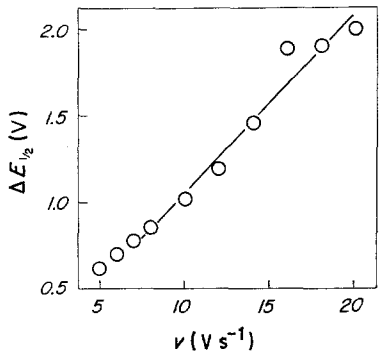

Fig. 14. Change of $\Delta E_{\frac{1}{2}}$ with v for peak a_1; $v > 8\,V s^{-1}$; $A = 0.8\,mm^2$.

sweep rates the formation of the film is controlled by diffusion, and at high sweep rates, by the electrical resistance in the pores of the film. Instant nucleation must occur with lateral growth.

The composition of the film cannot be determined electrochemically, but the data suggest that the passivation of tin is due to the formation of $Sn(OH)_4$ or SnO_2, a hypothesis supported by the literature [8]. The increasing stability of the film is due to the dehydration of $Sn(OH)_4$. The film can undergo rupture with metal exposure and further oxidation. In Fig. 15 the mechanism of the process is shown schematically.

Acknowledgements

Financial support from Financiadora de Estudos e Projetos (FINEP), Fundacão de Amparo à Pesquisa do Estado de São Paulo (FAPESP) (Procs. nos. 82/746-2; 86/2143-4), and Conselho Nacional de Desenvolvimento Cientifico e Tecnológico (CNPq) (Procs. nos. 301426/79; 300887/87; 130780/87) is gratefully acknowledged.

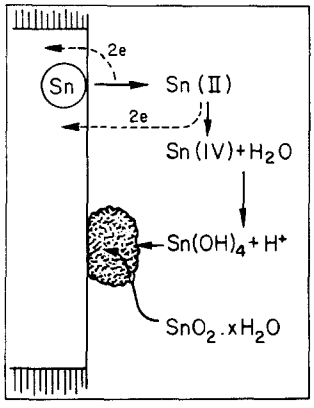

Fig. 15. Illustration of the dissolution-precipitation mechanism for tin.

References

[1] M. L. Varsányi, J. Jaén, A. Vértes and L. Kiss, *Electrochim. Acta* **30** (1985) 529.
[2] V. S. Muralidharan, K. Thangavel and K. S. Rajagopalan, *ibid.* **28** (1983) 1611.
[3] S. Kapusta and N. Hackerman, *J. Electrochem. Soc.* **129** (1982) 1886.
[4] *Idem., ibid.* **128** (1981) 327.
[5] *Idem., Electrochim. Acta* **25** (1980) 1625.
[6] *Idem., ibid.* **25** (1980) 949.
[7] *Idem., ibid.* **25** (1980) 1001.
[8] H. Do Duc and P. Tissot, *J. Electroanal. Chem.* **102** (1979) 59.
[9] T. Dickinson and S. Lotfi, *Electrochim. Acta* **23** (1978) 513.
[10] A. Vértes, H. Leidheiser Jr, M. L. Varsányi, G. W. Simmons and L. Kiss, *J. Electrochem. Soc.* **125** (1978) 1946.
[11] B. N. Stirrup and N. A. Hampson, *J. Electroanal. Chem.* **67** (1976) 45.
[12] *Idem., ibid.* **67** (1976) 57.
[13] S. A. Awad and A. Kassab, *ibid.* **26** (1970) 127.
[14] N. A. Hampson and N. E. Spencer, *Br. Corros. J.* **3** (1968) 1.
[15] M. Pugh, L. M. Warner and D. R. Gabe, *Corros. Sci.* **7** (1967) 807.
[16] A. M. Shams El Din and F. M. Abd El Wahab, *Electrochim. Acta* **9** (1964) 883.
[17] S. N. Shah and D. Eurof Davies, *ibid.* **8** (1963) 663.
[18] Y. M. Chen, T. J. O'Keefe and J. James, *Thin Solid Films* **129** (1985) 205.
[19] V. K. Gouda, E. N. Rizkalla, S. Abd El-Wahab and E. M. Ibrahim, *Corros, Sci.* **21** (1981) 1.
[20] M. S. Abdel Aal and A. H. Osman, *Corrosion NACE* **36** (1980) 591.
[21] A. Baraka, M. E. Ibrahim and M. M. Al-Abdallah, *Br. Corros. J.* **15** (1980) 212.
[22] B. N. Stirrup and N. A. Hampson, *J. Appl. Electrochem.* **6** (1976) 353.
[23] *Idem., J. Electroanal. Chem.* **73** (1976) 189.
[24] S. C. Britton and J. C. Sherlock, *Br. Corros. J.* **9** (1974) 96.
[25] R. Tunold and A. Broli, *Corros. Sci.* **13** (1973) 361.
[26] J. C. Sherlock and S. C. Britton, *Br. Corros. J.* **7** (1972) 180.
[27] A. R. Willey, *ibid.* 7 (1972) 29.
[28] J. C. Sherlock, J. H. Hancox and S. C. Britton, *ibid.* 7 (1972) 222.
[29] J. C. Sherlock and S. C. Britton, *ibid.* **8** (1973) 210.
[30] G. G. Kamm and A. R. Willey, *Corrosion* **17** (1961) 77t.
[31] E. L. Koehler, *J. Electrochem. Soc.* **103** (1956) 486.
[32] H. Leidheiser Jr., A. F. Rauch, E. M. Ibrahim and R. D. Granata, *ibid.* **129** (1982) 1651.
[33] T. F. Sharpe and S. G. Meibhur, *J. Chem. Educ.* **46** (1969) 103.
[34] C. A. T. V. Fazano, 'A Prática Mertalográfica', Hemus, São Paulo (1980).
[35] A. J. Calandra, N. R. de Tacconi, R. Pereiro and A. J. Arvia, *Electrochim. Acta* **19** (1974) 901.
[36] J. Kragten, 'Atlas of Metal Ligand Equilibria in Aqueous Solution', Ellis Horwood, Chester (1978) p. 623.
[37] A. E. Smith, *Analist* **98** (1973) 209.
[38] L. G. Sillen, *J. Chem. Ed.* **29** (1952) 600.
[39] D. A. Vermilyea, *J. Electrochem. Soc.* **110** (1963) 345.
[40] W. J. Müller, *Trans. Faraday Soc.* **27** (1931) 737.
[41] D. D. Macdonald, 'Transient Techniques in Electrochemistry', Plenum Press, New York (1977) chap. 8.